

## Imaging Spin-Reorientation Transitions in Consecutive Atomic Co Layers on Ru(0001)

Farid El Gabaly,<sup>1,\*</sup> Silvia Gallego,<sup>2</sup> Carmen Muñoz,<sup>2</sup> Laszlo Szunyogh,<sup>3</sup> Peter Weinberger,<sup>4</sup> Christof Klein,<sup>5</sup> Andreas K. Schmid,<sup>5</sup> Kevin F. McCarty,<sup>6</sup> and Juan de la Figuera<sup>1,†</sup>

<sup>1</sup>*Departamento de Física de la Materia Condensada and Centro de Microanálisis de Materiales, Universidad Autónoma de Madrid, Madrid 28049, Spain*

<sup>2</sup>*Instituto de Ciencia de Materiales de Madrid, CSIC, Madrid 28049, Spain*

<sup>3</sup>*Department of Theoretical Physics and Center for Applied Mathematics and Computational Physics, Budapest University of Technology and Economics, Budafoki út 8, H-1521 Budapest, Hungary*

<sup>4</sup>*Center for Computational Materials Science, Vienna University of Technology, Gumpendorferstrasse 1a, A-1060 Vienna, Austria*

<sup>5</sup>*Lawrence Berkeley National Laboratories, Berkeley, California 94720, USA*

<sup>6</sup>*Sandia National Laboratories, Livermore, California 94550, USA*

(Received 19 December 2005; published 11 April 2006)

By means of spin-polarized low-energy electron microscopy, we show that the magnetic easy axis of one to three atomic-layer thick cobalt films on Ru(0001) changes its orientation twice during deposition: One-monolayer and three-monolayer thick films are magnetized in plane, while two-monolayer films are magnetized out of plane. The Curie temperatures of films thicker than one monolayer are well above room temperature. Fully relativistic calculations based on the screened Korringa-Kohn-Rostoker method demonstrate that only for two-monolayer cobalt films does the interplay between strain, surface, and interface effects lead to perpendicular magnetization.

DOI: [10.1103/PhysRevLett.96.147202](https://doi.org/10.1103/PhysRevLett.96.147202)

PACS numbers: 75.30.Gw, 68.37.Nq, 68.55.-a, 75.70.Ak

Applications of ferromagnetic films depend on understanding and controlling the direction of the easy axis of magnetization. In particular, magnetization perpendicular to the film plane [1–4] holds promise for novel information-processing technologies [5]. Two important features of ultrathin films underlie this technological achievement: the high Curie temperature of transition metal films and the ability to control their microstructure. To provide deeper understanding, we study thin-film magnetism in a system whose components do not intermix, Co and Ru. Previous work [6,7] has shown that the easy axis of magnetization in Co/Ru multilayers changes from perpendicular at low Co thickness to in-plane for films thicker than 7 monolayers (ML) [8]. Because the Co films did not grow layer by layer [9,10], the films contained islands of varying thickness. Under these conditions, determining precisely how the magnetization changes as a function of film thickness is quite problematic.

Here we deposit Co films under conditions of perfect layer-by-layer growth. Then we use *in situ* spin-polarized low-energy electron microscopy (SPLEEM) [11–13] to locally determine the magnetization orientation of one-, two-, and three-monolayer thick Co films. We observe that the easy axis of magnetization changes after the completion of each atomic layer. By combining structural, morphological, and microscopic magnetic measurements with fully relativistic *ab initio* calculations based on the screened Korringa-Kohn-Rostoker (SKKR) [14] method, we explain the origin of the magnetization changes. Our results highlight that the magnetic anisotropy of ultrathin films is not simply explained by strain or interface effects alone but often by a combination of both effects.

The films are grown in two different ultrahigh vacuum low-energy electron microscopes (LEEM and SPLEEM) [11] by physical vapor deposition from calibrated dosers at rates of 0.3 ML/min. Details of the substrate-cleaning procedure as well as the experimental system are given elsewhere [15]. Perfect layer-by-layer Co growth occurs up to at least 7 ML when the Ru substrate has a low density of atomic steps [Figs. 1(a)–1(c)]. Because substrate steps

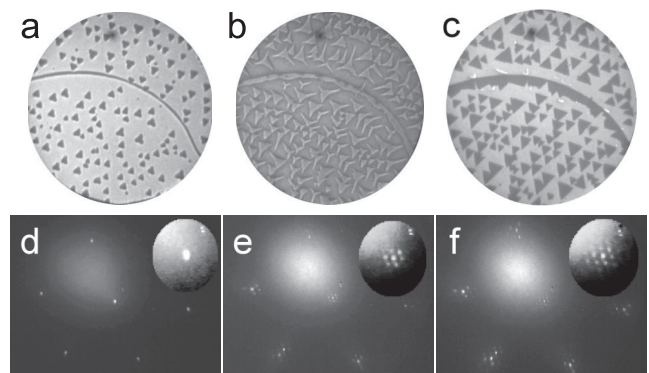


FIG. 1. LEEM images and diffraction patterns of a Co film growing on Ru(0001). (a)–(c) LEEM images show the morphology of the growing film. Field of view is 10  $\mu\text{m}$ , electron energy is 5 eV, and growth temperature is 460 K. One single, curved Ru step crosses the images. (a) 1 ML Co islands (dark) on Ru (light gray background). (b) 2 ML islands (light gray) on a complete 1 ML film (dark gray). (c) 3 ML islands (dark gray) on a nearly complete 2 ML film (light gray). (d)–(f) LEED patterns (70 eV) obtained from selected film areas of uniform thickness. Insets show magnified views of the specular beam. (d) 1 ML, (e) 2 ML, and (f) 3 ML of Co/Ru(0001).

enable a kinetic pathway to the nucleation of new film layers, three-dimensional growth [8,9] occurs after the first monolayer if substrate steps are present at even moderate density [16]. The film structure is determined by selected-area low-energy electron diffraction (LEED); i.e., the diffraction patterns were acquired with diffracted electrons coming from areas of the film with uniform thickness. One-monolayer films always present a  $1 \times 1$  LEED pattern indicating pseudomorphic growth; that is, the film has the same in-plane lattice parameter as the substrate [Fig. 1(d)]. Since the in-plane lattice parameter of bulk Co is 7.3% smaller than that of Ru, both measured within the hexagonal-close-packed (hcp) basal plane, the first monolayer of Co is under pronounced tensile strain. Analysis of the intensity versus energy curves of the specular and integer diffraction spots (not shown) establishes that the Co film continues the hcp stacking [17] of the substrate, with a Co-Ru interplanar separation estimated to be contracted 6% relative to the Ru-Ru interplanar spacing. For films thicker than 1 ML, satellite spots appear around the bulk diffraction beams [Figs. 1(e) and 1(f)]; i.e., the thicker films are no longer pseudomorphic. From the diffraction patterns, we estimate that the in-plane spacing of 2 and 3 ML Co films is  $5 \pm 1\%$  less than the Ru spacing, leaving the film strained only by 3% relative to the bulk-Co value. At intermediate coverages between 1 and 2 ML, the 1 ML areas are still pseudomorphic, as detected by dark-field imaging [15], while 2 ML islands are relaxed and 3 ML films grow mainly in a face-centered-cubic structure.

To characterize the easy axis of magnetization, we employ SPLEEM [13]. With this technique, the magnetization can be mapped onto three orthogonal directions [18]: The absence of contrast in the images (gray) indicates no magnetization component along the selected direction; bright and dark areas indicate a component of the magnetization along or opposed to the illuminating beam polarization, respectively. In Fig. 2, we show LEEM and SPLEEM images of a film that consists of a complete monolayer of Co plus some second layer islands [Fig. 2(d)], both in the middle of the substrate terraces and at the bottom of the ruthenium substrate steps. The SPLEEM images show the spatially resolved component of the magnetization in three orthogonal directions: two in plane [Figs. 2(b) and 2(c)] and one out of plane [Fig. 2(a)]. In one-monolayer areas, the magnetization is oriented in the plane of the film, while for two layer islands the magnetization is out-of-plane. For a complete 2 ML film with additional 3 ML islands (Fig. 3), the magnetization of the 2 ML areas is out-of-plane. In contrast, 3 ML thick islands and thicker films (not shown) are magnetized in plane. To summarize, two magnetization easy-axis reorientation transitions are found in three consecutive atomic layers: at the crossover between 1 and 2 ML and between 2 and 3 ML. This behavior has also been confirmed in films devoid of islands. We do not find intermediate easy-axis orientations (i.e., in between in plane and out of plane), such as observed for Co films on other substrates [19,20].

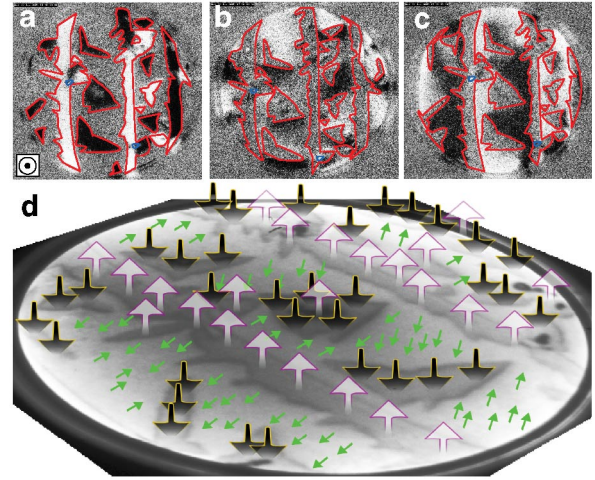


FIG. 2 (color). Images of topography and magnetization of one region of a 1.5 ML Co/Ru(0001) film. Images were taken at 110 K. Field of view is  $2.8 \mu\text{m}$  and electron energy is 7 eV. (a)–(c) SPLEEM images with electron-polarization oriented: (a) out of plane; (b) in plane and  $13^\circ$  off a compact direction; (c) in plane and  $103^\circ$  off a compact direction. 2 ML islands are framed in red (two small 3 ML islands are framed in blue). (d) LEEM image of the surface with the deduced magnetization direction indicated by arrows (black and white arrows mean out-of-plane magnetization; green arrows mean in-plane magnetization). Dark gray indicates 2 ML islands, light gray 1 ML film.

The Curie temperature of the films changes dramatically from the first layer to the second. The first layer has a Curie temperature close to 170 K, as detected by the loss of magnetic contrast in the 1 ML areas. The Curie temperature of the 2 ML islands, which are magnetized out of plane, is well above room temperature, about 470 K. Thicker films exhibit Curie temperatures above 470 K. Iron films on W(110) [21,22] also present a double spin-reorientation transition but with a Curie temperature well below room temperature for out-of-plane magnetization [23]. In this particular system, strain did not drive the reorientation transitions [23,24].

The anisotropy energy that governs the orientation of the easy axis of magnetization is the result of a delicate balance between different contributions. In thin films, the dominating term is often the dipolar or shape anisotropy. This contribution, which results from the long-range magnetic dipole-dipole interactions, favors an in-plane orientation of the magnetization. However, other contributions such as the bulk, interface, and surface magnetocrystalline anisotropy energies, as well as magnetoelastic terms [25,26], can compete with the dipolar anisotropy energy and can favor out-of-plane magnetization. To understand the effects that give rise to the observed changes in the orientation of the Co magnetization, we perform *ab initio* calculations in terms of the SKKR method [14]. Changing the lattice parameters in the calculations allows us to determine how strain influences the magnetic anisotropy. The magnetic anisotropy energy (MAE) is calculated as

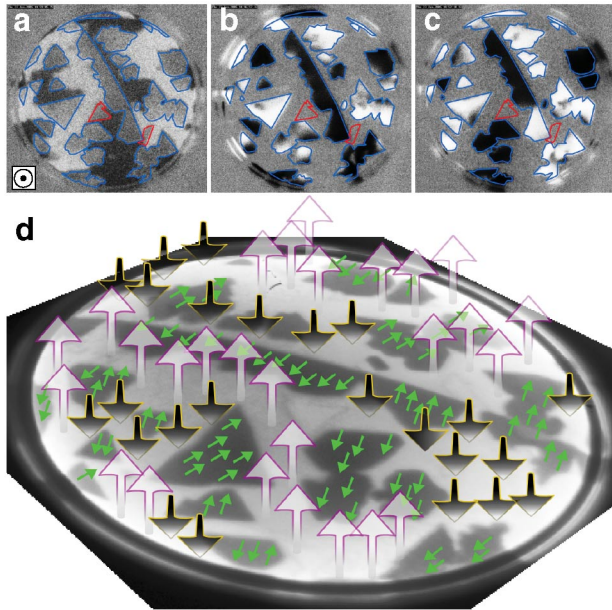


FIG. 3 (color). Images of topography and magnetization of one region of a 2.5 ML Co/Ru(0001) film. Images were taken at room temperature. Field of view is  $2.8 \mu\text{m}$  and electron energy is 7 eV. (a)–(c) SPLEEM images with electron-polarization oriented: (a) out of plane; (b) in plane and  $13^\circ$  off a compact direction; (c) in plane and  $103^\circ$  off a compact direction. 3 ML islands are framed in blue. Two vacancy islands in the 2 ML area, where Co is 1 ML thick, are framed in red. (d) LEEM image of the surface with the deduced magnetization direction indicated by arrows (black and white arrows mean out-of-plane magnetization; green arrows mean in-plane magnetization). Dark gray indicates 3 ML islands, light gray 2 ML film.

the difference of the total energy for in-plane and out-of-plane magnetization. A positive MAE corresponds to out-of-plane magnetization. By employing the force theorem [27], the MAE is defined as the sum of a band energy  $\Delta E_b$  and a magnetic dipole-dipole energy term  $\Delta E_{dd}$ . The band-energy term can be further resolved into contributions with respect to atomic layers that enable us to define surface and interface anisotropies.

First, we calculate the anisotropy of the pseudomorphic one-monolayer Co films, taking into account contractions of the Co-Ru interlayer distance ( $d$ ). As summarized in Fig. 4(a), the value of  $\Delta E_b$  increases as the interplanar spacing decreases; however, due to the negative  $\Delta E_{dd}$ , the preferred orientation of the magnetization remains always in plane. Interestingly, the change in MAE is not proportional to the strain, and, therefore, simple magnetoelastic arguments do not apply. Furthermore, we also tested the effect of contracting the in-plane lattice parameter of the substrate and film. In that case, the MAE does not change significantly (result not shown in the figure). We conclude that the magnetization of the monolayer remains in plane regardless of strain.

For two-monolayer and thicker films, the in-plane separation of the Co atoms is contracted by  $\sim 5\%$  with respect

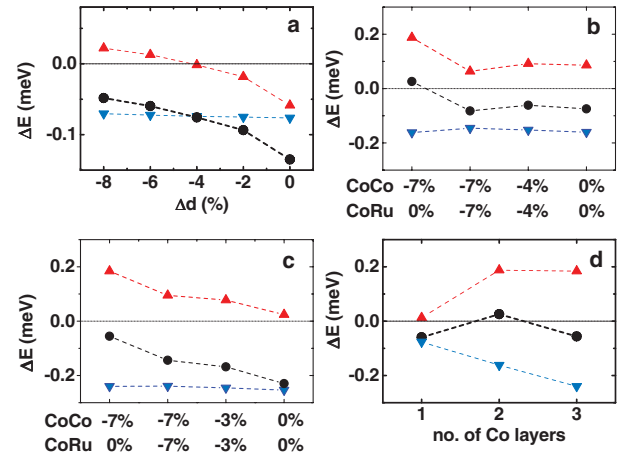


FIG. 4 (color). Calculated magnetic anisotropy energies of the different Co films on Ru. (a)–(c) Dependence of the calculated MAE on the interlayer distance referred to the substrate interlayer spacing. MAE (black circle) and its components  $\Delta E_b$  (red up triangle) and  $\Delta E_{dd}$  (blue down triangle) for: (a) a pseudomorphic 1 ML Co/Ru(0001) film under different contractions of the Co-Ru interlayer distance; in-plane strained (b) 2 ML Co/Ru(0001) and (c) 3 ML Co/Ru(0001) films with either the same or different (data points labeled by CoCo  $-7\%$  and CoRu  $0\%$ ) Co-Co and Co-Ru interlayer separations. (d) MAE and its components in the most realistic geometry for the 1, 2, and 3 ML Co films on Ru(0001), displaying the double reorientation transition.

to the Ru structure, leading to a  $20 \times 20$  coincidence lattice. We model the in-plane relaxation by contracting the supporting Ru substrate together with the Co film. Under this assumption, taking the same contraction for the Co-Co and Co-Ru interlayer spacing  $d$  from 0 to  $7\%$  relative to the substrate interlayer distance leads to a positive value of  $\Delta E_b$  [Fig. 4(b)] that, however, does not compensate the negative  $\Delta E_{dd}$ . For the bilayer, the observed positive sign of the MAE occurs when different values for the Co-Co and Co-Ru interlayer distances are considered. In order to estimate the preferred relaxation of the interlayer distances, we assume that atoms try to maintain the nearest-neighbor distances of their bulk materials, with Co-Ru distances being an average of the preferred Co-Co and Ru-Ru interlayer distances. This leads to contractions of  $7\%$  for the Co-Co interlayer distances and a nearly unrelaxed Co-Ru spacing. As shown in Fig. 4(b) (leftmost data points), such a lattice distortion considerably increases  $\Delta E_b$  resulting in a total positive MAE. A positive MAE is also obtained for an ideal Ru lattice with Co interlayer distances contracted by more than  $4\%$  (not shown). In 3 ML thick films, nonuniform contractions of the Co layers lead also to an enhancement of the positive  $\Delta E_b$  [Fig. 4(c)]. Nevertheless, the decrease in the  $\Delta E_{dd}$  term associated with thicker films drives the magnetization in plane. A summary of our calculations of the MAE for the Co films of different thickness, each at the most likely geometry, is shown in Fig. 4(d). As a function of thickness, the MAE changes sign twice, as observed experimentally.

Our calculations show that the double spin-reorientation transition is the result of a complicated interplay of structural and interface/surface electronic effects. All contributions to  $\Delta E_b$  are strongly influenced by structural modifications. For 2 ML thick films with the same Co-Co and Co-Ru interlayer separation, the dominant term is  $\Delta E_b$  related to the interface Co. However, when Co-Co and Co-Ru separations are allowed to be different, the contribution of the surface Co layer is remarkably enhanced resulting in a positive value of the MAE (out-of-plane magnetization).

In conclusion, we deposited films of Co onto Ru(0001) in the thickness range of up to 3 atomic monolayers and find that the Curie temperature is well above room temperature, provided the thickness is more than a single atomic monolayer. We observe two sharp reorientation transitions of the magnetization: 1 ML as well as 3 ML or thicker Co films have an in-plane easy axis, while only 2 ML thick films are magnetized in the out-of plane direction. The first transition is associated with a structural transformation from laterally strained, pseudomorphic 1 ML thick films to relaxed 2 ML thick films. Our first principles calculations show that the in-plane easy axis of one- and three-monolayer films is stable with respect to variations of the strain conditions. Only for two-monolayer films does the combination of strain with additional interface and surface effects drive the magnetic easy axis into the out-of-plane direction.

This research was partly supported by the U.S. Department of Energy under Contracts No. DE-AC02-05CH11231 and No. DE-AC04-94AL85000, by the Spanish Ministry of Science and Technology under Projects No. MAT2003-08627-C02-02, No. MAT2003-04278, and No. 2004-HU0010, and by the Comunidad Autónoma de Madrid under Project No. GR/MAT/0155/2004. Additional support by the Hungarian Scientific Research Fund (OTKA T037856 and T046267) and the Austrian Ministry of Labor and Economy (bw:aw 98.366) is acknowledged. S.G. acknowledges support through a “Ramón y Cajal” contract from the Spanish Ministry of Education and Science.

---

\*Electronic addresses: farid.elgabaly@uam.es  
<http://hobbes.fmc.uam.es/loma>

†Electronic address: juan.delafiguera@uam.es

- [1] U. Gradmann, Appl. Phys. **3**, 161 (1974).
- [2] P.F. Carcia, A.D. Meinhardt, and A. Suna, Appl. Phys. Lett. **47**, 178 (1985).
- [3] B.N. Engel, C.D. England, R.A. Van Leeuwen, M.H. Wiedmann, and C.M. Falco, Phys. Rev. Lett. **67**, 1910 (1991).
- [4] M.T. Johnson, P.J.H. Bloemen, F.J.A.d. Broeder, and J.J.d. Vries, Rep. Prog. Phys. **59**, 1409 (1996).
- [5] C. Chappert *et al.*, Science **280**, 1919 (1998).
- [6] K. Ounadjela, D. Muller, A. Dinia, A. Arbaoui, P. Panissod, and G. Suran, Phys. Rev. B **45**, 7768 (1992).
- [7] C.L. Dennis *et al.*, J. Phys. Condens. Matter **14**, R1175 (2002).
- [8] D. Muller, K. Ounadjela, P. Venegues, V. Pierron-Bohnes, A. Arbaoui, J.P. Jay, A. Dinia, and P. Panissod, J. Magn. Magn. Mater. **104–107**, 1873 (1992).
- [9] C. Liu and S.D. Bader, J. Magn. Magn. Mater. **119**, 81 (1993).
- [10] H.F. Ding, A.K. Schmid, D. Li, K.Y. Guslienko, and S.D. Bader, Phys. Rev. Lett. **94**, 157202 (2005).
- [11] E. Bauer, Rep. Prog. Phys. **57**, 895 (1994).
- [12] T. Duden and E. Bauer, Rev. Sci. Instrum. **66**, 2861 (1995).
- [13] T. Duden and E. Bauer, Surf. Rev. Lett. **5**, 1213 (1998).
- [14] J. Zabloudil, R. Hammerling, L. Szunyogh, and P. Weinberger, *Electron Scattering in Solid Matter: A Theoretical and Computational Treatise* (Springer-Verlag, Berlin, 2005).
- [15] F. El Gabaly, W.L.W. Ling, K.F. McCarty, and J. de la Figuera, Science **308**, 1303 (2005).
- [16] W.L. Ling, T. Giessel, K. Thurmer, R.Q. Hwang, N.C. Bartelt, and K.F. McCarty, Surf. Sci. **570**, L297 (2004).
- [17] R.Q. Hwang, C. Günther, J.S. Günther, E. Kopatzki, and R.J. Behm, J. Vac. Sci. Technol. A **10**, 1970 (1992).
- [18] R. Ramchal, A.K. Schmid, M. Farle, and H. Poppa, Phys. Rev. B **69**, 214401(R) (2004).
- [19] H. Fritzsche, J. Kohlhepp, and U. Gradmann, Phys. Rev. B **51**, 15 933 (1995).
- [20] T. Duden and E. Bauer, Phys. Rev. Lett. **77**, 2308 (1996).
- [21] H.J. Elmers, J. Hauschild, and U. Gradmann, Phys. Rev. B **59**, 3688 (1999).
- [22] O. Pietzsch, A. Kubetzka, M. Bode, and R. Wiesendanger, Science **292**, 2053 (2001).
- [23] K. von Bergmann, Ph.D. thesis, Hamburg, 2004.
- [24] J. Prokop, A. Kukunin, and H.J. Elmers, Phys. Rev. Lett. **95**, 187202 (2005).
- [25] D. Sander, Rep. Prog. Phys. **62**, 809 (1999).
- [26] D. Sander, J. Phys. Condens. Matter **16**, R603 (2004).
- [27] H.J.F. Jansen, Phys. Rev. B **59**, 4699 (1999).